

PAPER • OPEN ACCESS

## Design and application of a reflective programmable metasurface element in C Band

To cite this article: H S Hou *et al* 2019 *IOP Conf. Ser.: Mater. Sci. Eng.* **479** 012040

View the [article online](#) for updates and enhancements.



**IOP | ebooks™**

Bringing you innovative digital publishing with leading voices to create your essential collection of books in STEM research.

Start exploring the collection - download the first chapter of every title for free.

# Design and application of a reflective programmable metasurface element in C Band

H S Hou<sup>1</sup>, X J Gao, L Zhu, P Xie and C B Zhang

Air and Missile Defense College, Air Force Engineering University, Xi'an 710051, China

<sup>1</sup> E-mail: 451352290@qq.com

**Abstract.** The programmable metasurface element is able to achieve continuous controllable responses by loading controllable electronic devices. In this work, a reflective programmable element working at 5GHz is implemented with varactor diodes. By tuning the biasing DC voltage loaded on the varactor diodes, the capacitance can be changed, and then the reflected phases can be tuned. Simulated results show that the reflected phase can cover the 360° and amplitude of the reflective wave is more than 0.7. In order to verify the property of the proposed element, a reflective electronically controllable metasurface is designed based on the proposed element. The metasurface is able to steer the reflective wave from -30° to 30°. The proposed element possesses distinctive features such as simple ultrathin structure, programmable control, and subwavelength, thus exhibiting the promising prospects in agile antennas.

## 1. Introduction

Recently, metamaterials as artificial composite microstructures scale have received tremendous attention because their electromagnetic(EM) properties can be controlled at will. Compared with bulk metamaterials [1-3], metasurfaces(MSs) [4-19] consisting of a set of subwavelength resonant structures with different geometrical parameters have the advantages of easy fabrication, thin thickness and low loss. As a kind of MSs, phase gradient metasurface (PGMS) is an artificial surface which has been proposed by Yu et al. to demonstrate the general Snell's law [4]. Due to extraordinary abilities to manipulate phase and amplitude of EM waves, PGMS attracts increasing attention in polarization conversion and beam steering, resulting in fascinating effects such as anomalous reflection/refraction [5-7], focusing EM waves [8-11] and polarization conversion [12-15]. However, most metasurfaces are designed and fabricated without active elements. And the functionalities could not be changed sometimes, leading to the low freedom of designing multifunctional devices.

In recent years, more efforts have been devoted to achieve real-time control of metasurfaces by considering tunable or switchable meta-atoms driven by mechanically actuation or electric voltage bias [16-19]. Compared with mechanic ally actuation, programmable metasurfaces, or digital metasurfaces [20], which are proposed by Cui et al., have distinct abilities for manipulating EM waves at real-time continuous and various reprogrammable functions in one thin-thickness metasurface. Moreover, it should be distinguished from conventional phase antenna arrays, which can actively shape the radiation patterns by controlling each emitter but with much more complex, bulky and highly expensive phase shifters and feeding networks [21]. These special metasurfaces may greatly simplify the design and improve the flexibility of specific device functionalities.

In order to have full control of the reflection phase, programmable element with full 360 degree phase tuning range is often desired within a frequency band. Compared with passive element without loading tunable meta-atoms, active element is not easy to obtain full 360 degree phase tuning range. Due to the finite tuning range of the parameters of the practical active component, such as the junction capacitance of the varactor, the shift of the resonance frequency and the reflection phase curve are always finite. Moreover, the asymptotic behavior [22] of the reflection phase at 180 degree always exist in the conventional structures with single resonance. Therefore, 360 degree full phase tuning range usually can not be obtained.

To solve above problems, the authors proposed a kind of multipole active element with two resonance poles and one resonance zero in between. Owing to two resonance connected to each other, the reflection phase can cover the whole 360 degree tuning range without the asymptotic behavior. Therefore, the full 360 degree control can be achieved by controlling the varactors capacitance with tuning the bias voltage.

## 2. Design of unit cell

We design a reflective-type element with geometrical details shown in Figure 1. As can be seen, the element is composed of three metallic layers sandwiched by two dielectric layers: the top composite metallic pattern ( $p=12\text{mm}$ ,  $w_1=4\text{mm}$ ,  $w_2=3.2\text{mm}$ ,  $w_3=3.2\text{mm}$ ,  $w_4=5.1\text{mm}$ ,  $e_1=1\text{mm}$ ,  $e_2=0.5\text{mm}$ ,  $h_1=3\text{mm}$ ,  $h_2=0.65\text{mm}$ ,  $R=4.5\text{mm}$ ), middle ground plane and the bottom feeding network. The dielectric spacer is F4B (poly tetra fluoroethylene glass cloth board,  $\epsilon_r=2.65$ ,  $h=3\text{mm}$  and loss tangent 0.001) and TP-2 (microwave composite dielectric copper clad substrate TP-2,  $\epsilon_r=9.6$ ,  $h=0.65\text{mm}$  and loss tangent 0.001). As the presence of the middle ground plane, a completely reflective system without transmissions is achieved. To break the asymptotic behavior, the element is designed as a double resonance unit cell. When illuminated by normally incident  $y$ -polarized EM waves along  $z$  direction, the middle and side patch couple to the ground and generate independent magnetic resonance around  $f_1$  and  $f_2$  respectively, evidenced by the dips in the finite-difference-time-domain (FDTD) simulated  $y$ -polarized reflection spectrum depicted in Figure 2. Therefore, the whole 360 degree phase difference is easy obtained.

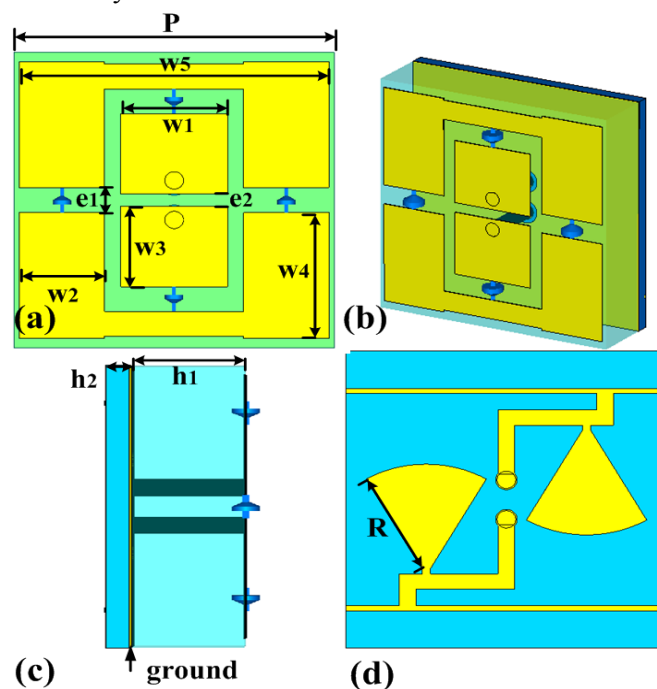


**Figure 1.** Structure of the unit cell and the simulated setup. (a) top view, (b) perspective view, (c) side view, (d) back view.

Here, varactor diode (SMV2019-079LF, Skyworks Solutions Inc.) is actualized with the gap of the metallic patch as Figure 1 shown. The external voltages are imposed to the diodes through two metallic vias. By tuning the bias voltages, the reflection phase can be controlled. The equivalent CM(circuit model) for the varactor diode SMV 2019-079LF is shown as Figure 2(a). In our FDTD simulations ,we replaced the varactor diode by a series resonant tank with inductance  $L_v=0.7\text{nH}$ , resistance  $R_v=4.8\ \Omega$ , and capacitance  $C_v(0.30\text{pF}-2.22\text{pF})$ , which sensitively depends on the voltage  $V$  imparted on it through a  $C_v\sim V$  curve provided by data sheet of SMV 2019-079LF. Figure 3 depicts the reflection phase and amplitude versus the capacitance  $C_v$  at 5GHz.

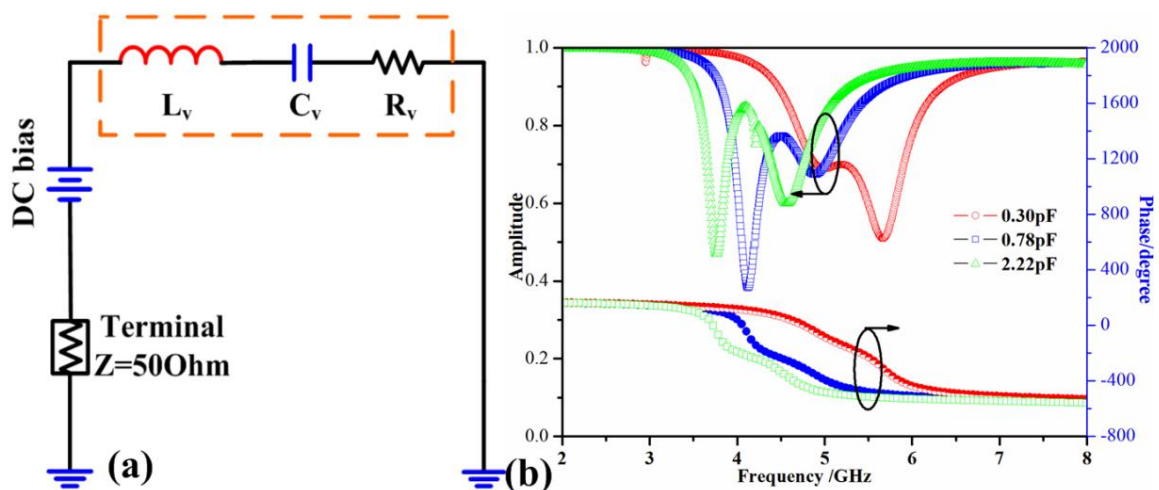


**Figure 2.** (a) The equivalent circuit model for the varactor diode SMV2019-079LF, (b) FDTD simulated spectra of reflectance and reflection phase of the proposed element under different  $C_v$ .

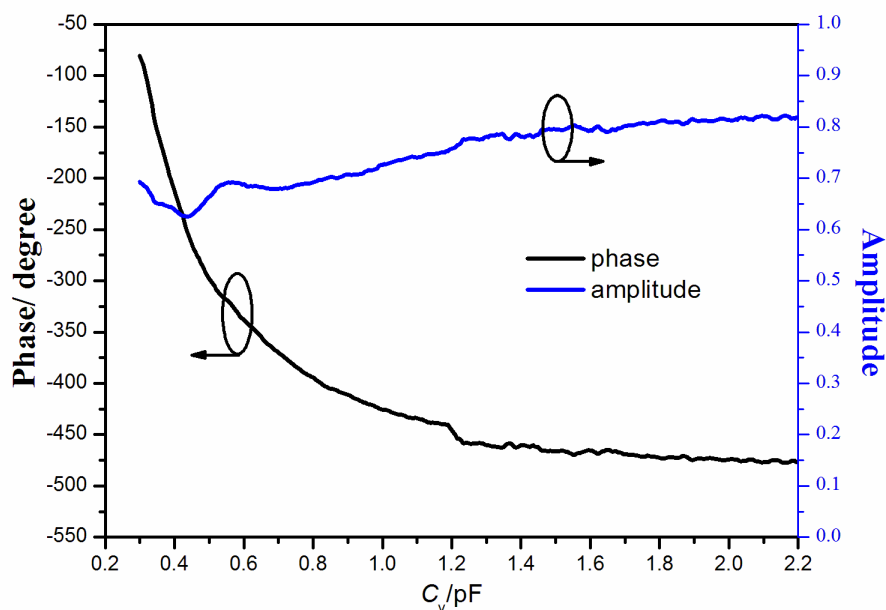


**Figure 3.** Reflection phase and amplitude versus the capacitance  $C_v$  at 5GHz.

### 3. Design of programmable metasurface and its application

As we all know, the reflected wave will always deflect to the phase delay direction according to the general refraction law [3] as depicted in equation (1)

$$n_r \sin(\theta_r) - n_i \sin(\theta_i) = \frac{\lambda}{2\pi} \frac{d\varphi}{dx} \quad (1)$$

where  $\varphi$  is the phase discontinuity at a local position on the metasurface,  $\theta_r$  ( $\theta_i$ ) is the reflected (incident) angle of the EM waves,  $n_r$  ( $n_i$ ) is the refracted index of the reflective (incident) medium and  $\lambda$  is the wavelength. In the design, EM wave normally impinges on unit cells, thus  $\theta_i$  is denoted by 0. Considering that the unit cell is placed in free space (i.e.,  $n_i=1$ ), we can obtain the refraction angle  $\theta_r$  as depicted in equation (2)

$$\theta_r = \sin^{-1} \left( \frac{\lambda}{2\pi} \times \frac{d\varphi}{dx} \right) \quad (2)$$

Based on above designed procedure, one-dimensional programmable metasurface with inverse linear phase gradient along  $x$  direction for  $y$ -polarization has been designed. As shown in Figure 4, the programmable metasurface is composed of 1\*15 unit cells which are completely same. To observe the programmable anomalous reflection, different phase gradient has been designed in the Table 1. The calculated anomalous reflective angle can be obtained from equation (2). By tuning the  $C_v$  of varactor etched in the unit cells of the programmable metasurface, different phase gradient shown in Table 1 can be easily realized. According to Figure 3, we can choose different  $C_t$  at will.

**Table 1.** calculated/simulated anomalous reflective angle.

phase gradient $\Delta\Phi$	calculated anomalous reflective angle	simulated anomalous reflective angle
45°	38.7°	38.5
30°	24.6°	24.3
0°	0°	0
-30°	-24.6°	-24.3
-45°	-38.7°	-38.5

To validate the proposed programmable metasurface's function of programmable anomalous reflection, we simulate the metasurface in CST Microwave Studio. As Figure 4 shown, the programmable metasurface is perpendicularly illuminated by a  $y$ -polarized plane wave along  $z$  direction in CST Microwave Studio, in which open boundary condition is set along  $x/z$  direction and periodic boundary condition is set along  $y$  direction. When the programmable metasurface with different phase gradient in the Table 1 is normally impinged by plane waves, the 3D-farfields are calculated as shown in Figure 5(a)-(e). To clearly show the reflected angles for  $y$ -polarized waves, the normalized farfield patterns in polar are depicted in Figure 5(f). As illustrated in this figure, the reflection angles for  $y$ -polarized beams are denoted by 38.6°, 24.4°, 0°, -24.5°, -38.5° along  $+x$  direction, which are in good accordance with theoretic ones calculated by equation (2).

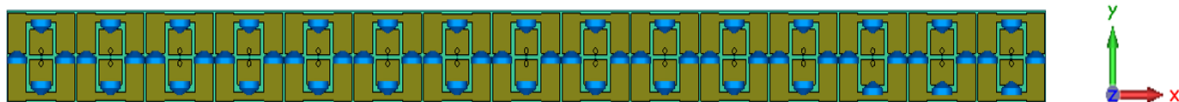


**Figure 4.** Structure of the proposed programmable metasurfaces.

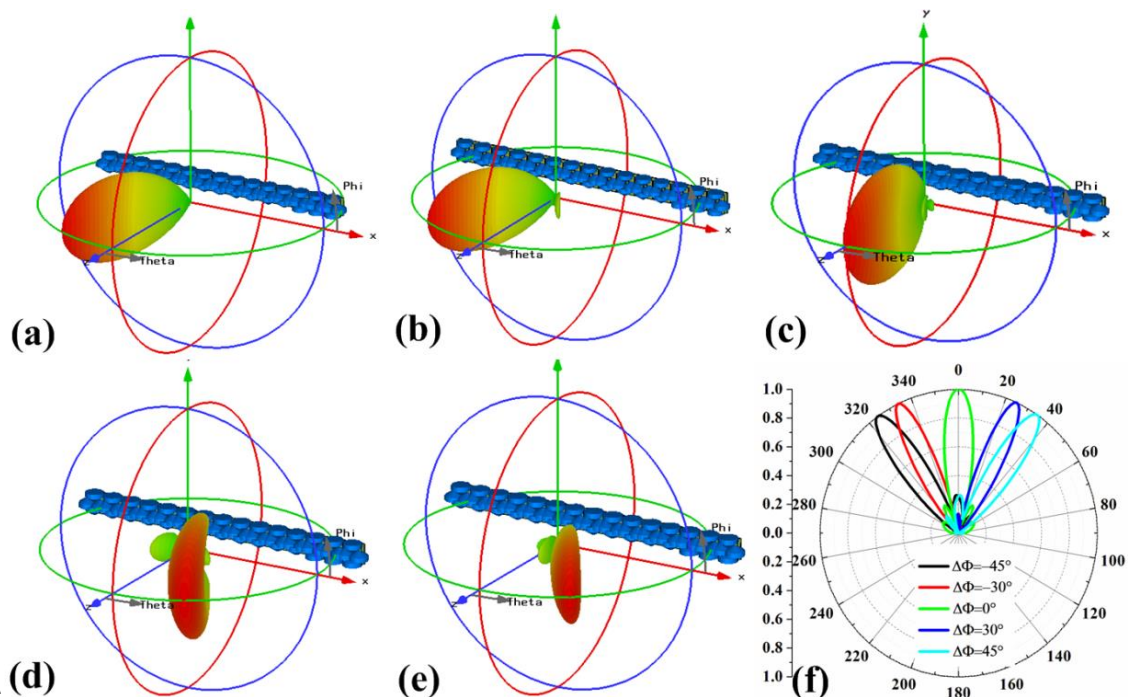


**Figure 5.** Simulated anomalous reflection farfield pattern (a) $\Delta\Phi=-45^\circ$ , (b) $\Delta\Phi=-30^\circ$ , (c) $\Delta\Phi=0^\circ$ , (d) $\Delta\Phi=30^\circ$ , (e) $\Delta\Phi=45^\circ$ , (f) the normalized farfield patterns.

#### 4. Conclusions

In conclusion, we proposed a reflective programmable element in C band and designed programmable anomalous reflection metasurface with the proposed element at 5 GHz. In our proposed configuration, different anomalous reflective angles can be obtained at the same working frequency. Results show that the calculated results convince the simulated results well. The proposed element possesses distinctive features such as simple ultrathin structure, programmable control, and subwavelength, thus exhibiting the promising prospects in agile antennas.

#### References

- [1] Shi Y, Yang K D, Yang Y X and Ma Y L 2015 Chin. Phys. B **24** 44102
- [2] Liu G C, Li C and Fang G Y 2015 Chin. Phys. B **24** 14101
- [3] Liu C and Wang Y H 2015 Chin. Phys. B **24** 10602
- [4] Yu N F, Genevet P, Kats M A, Aieta F, Tetienne J P, Capasso F and Gaburro Z 2011 Science **334** 333-337
- [5] Pu M B, Chen P, Wang C T, Wang Y Q, Zhao Z Y, Hu C G, Huang C and Luo X G 2013 AIP Advances **3** 052136
- [6] Wei Z Y, Cao Y, Su X P, Gong Z J, Long Y and Li H Q 2013 Opt. Express **21** 010739
- [7] Ni X, Ishii S, Kildishev A V and Shalaev V M 2013 Light Sci. Appl. **2** 72
- [8] C. Saiedi, D. van der Weide, 2014 Appl. Phys. Lett., **105** 053107
- [9] Pors A, Nielsen M G, Eriksen R L, and Bozhevolnyi S I 2013 Nano Lett. **13** 829-834
- [10] Li X, Xiao S Y, Cai B G, He Q, Cui T J and Zhou L 2012 Opt. Lett. **37** 4940-4942
- [11] Kuznetsov S A, Astafev M A, Beruete M and Navarro-Ci'a M 2015 Srep. **5** 07738
- [12] Ma W, Jia D L, Yu X M, Feng Y and Zhao Y J 2016 Appl. Phys. Lett. **108** 071111
- [13] Song K, Liu Y H, Luo C R and Zhao X P 2014 J. Phys. D:Appl. Phys. **47** 505104
- [14] Chen H Y, Wang J F, Ma H, Qu S B, Xu Z, Zhang A X, Yan M B and Li Y F 2014 J. Appl. Phys. **115** 154504
- [15] Zhu H L, Cheung S W, Chung K L and Yuk T I 2013 IEEE T. ANTENN. PROPAG. **61** 4615-

4623

- [16] Xu H X, Ma S J, Luo W J, Cai T, Sun S L, He Q and Zhou L 2016 Appl. Phys. Lett. **108** 021110
- [17] Yang H H, Cao X Y, Yang F, et.al. 2016 Sci. Rep. **6** 35692
- [18] Li, Y. et al. 2016 Sci. Rep. **6** 23731
- [19] Wan X, Qi M Q, Chen T Y and Cui T J 2016 Sci.Rep. **6** 20663
- [20] Cui T J, Qi M Q, Wan X, Zhao J and Cheng Q 2014 Light:Sci. Appl. **3** e218
- [21] Chen K , Feng Y J, et al. 2017 Adv. Mater. **7** 42802
- [22] Zhu B, Zhao J and Feng Y 2013 Sci. Rep. **3** 3059